NCAR-TN/STR-85
NCAR TECHNICAL NOTE

July 1973

A Microfilm Atlas of Magnetic Fields in the Solar Corona

Gordon Newkirk, Jr.
Dorothy E. Trotter
Martin D. Altschuler
High Altitude Observatory
Robert Howard
Hale Observatories

HIGH ALTITUDE OBSERVATORY

NATIONAL CENTER FOR ATMOSPHERIC RESEARCH
BOULDER, COLORADO

FOREWORD

The work reported here is a cooperative study by the High Altitude Observatory (HAO) of NCAR and the Hale Observatories of the Carnegie Institution of Washington and the California Institute of Technology. Photospheric data used to construct the Atlas were obtained in a program supported in part by the Office of Naval Research under Contract NR013-230, N000 14-66-C-0239. Most of the observations were made by Thomas A. Cragg, John M. Adkins, and Merwyn G. Utter of the Hale Observatories. The authors wish to express gratitude to Thomas Wilson of HAO for carrying out many of the programming and computational procedures which made the Atlas possible. The Atlas is available on 35-mm microfilm for $50; orders should be addressed to D. E. Trotter, HAO.

Gordon Newkirk Jr.
Dorothy E. Trotter
Martin D. Altschuler
High Altitude Observatory
Boulder, Colorado

Robert Howard
Hale Observatories
Pasadena, California

April 1973

CONTENTS

Foreword iii

I. INTRODUCTION 1

II. MATHEMATICAL PROCEDURE 2

III. DATA 2

IV. LIMITATIONS 5

A. Error-Free Approximation 6
B. Truncation of the Polynomial 9
C. Limited Data Coverage 12
D. Magnetograph Saturation 13
E. Polar Fields 17

V. USING THE ATLAS 18

VI. EXTENSIONS OF THIS ATLAS 22

References 23

I. INTRODUCTION

It has become increasingly apparent in the past several years that magnetic fields are important to the dynamics of many phenomena of the solar corona, of the interplanetary medium, and of the interaction of the interplanetary plasma with the earth and other planets. Recent research efforts have tried to clarify the connection between the coronal density structure and the coronal magnetic field (e.g. Saito and Billings, 1962; Newkirk, et al., 1968; Schatten, et al., 1969; Altschuler and Newkirk, 1969; Newkirk and Altschuler, 1970; Bohlin, 1970; Pneuman and Kopp, 1970; Martres, et al., 1970; Schatten, 1971; Newkirk, 1971), between radio burst events and the configuration of the field (Smerd and Dulk, 1970; Lantos-Jarry, 1970; Dulk, et al., 1971; Dulk and Altschuler, 1971; McCabe, 1971) and between various interplanetary phenomena and the coronal field (Schatten, 1970; Valdez and Altschuler, 1970).

Progress over a wide range of problems in solar physics and solar terrestrial studies requires detailed knowledge of the coronal magnetic field. Routine direct measurements of the magnetic field of the corona, however, are still in the future. At present, therefore, we must calculate the coronal magnetic field from measurements of the photospheric magnetic field without knowing for certain how closely the calculated field approximates the actual field. Such calculations can be used to interpret measurements of many phenomena known to be related to coronal magnetic fields; and together with coronal observations these calculations should increase our overall knowledge of coronal physics.

The Atlas comprises 11,000 microfilm maps of the calculated potential (or current-free) magnetic fields of the solar corona between August 1959

and June 1970. For each solar rotation in this interval, there are two sets of maps. The first set of maps (see Fig. 1) shows the geometry of the coronal magnetic field but includes field lines originating from both strong or weak fields at the photosphere. (However, no field lines are drawn from a photospheric region if the calculated field strength there is less than 0.08 Gauss.) The second set of maps (see Fig. 2) shows field lines which emanate from the regions of strongest photospheric magnetic field. Each set provides one map for every 10^{o} interval of solar longitude or 36 maps for each rotation.

II. MATHEMATICAL PROCEDURE

The mathematical procedure used in calculating the potential (or current-free) coronal magnetic field from measurements of the photospheric magnetic field is discussed in Altschuler and Newkirk (1969), hereafter denoted Paper I. The relevant equations are derived in Sections 4, 6, and 8 of that paper; the limitations of the potential field calculations and the treatment of the available data are discussed in Sections 2 and 10; a brief description of the computer technique is given in Section 9. Paper I should be examined in detail before applying the Atlas to practical problems.

III. DATA

The line-of-sight photospheric fields are determined by measuring the Zeeman splitting of the lines λ525.0216 nm of FeI and λ524.7574 nm of CrI using the Mt. Wilson magnetograph with a square aperture of dimensions 23 arcsec x 23 arcsec. After June 16, 1966, only the λ525.0261 nm

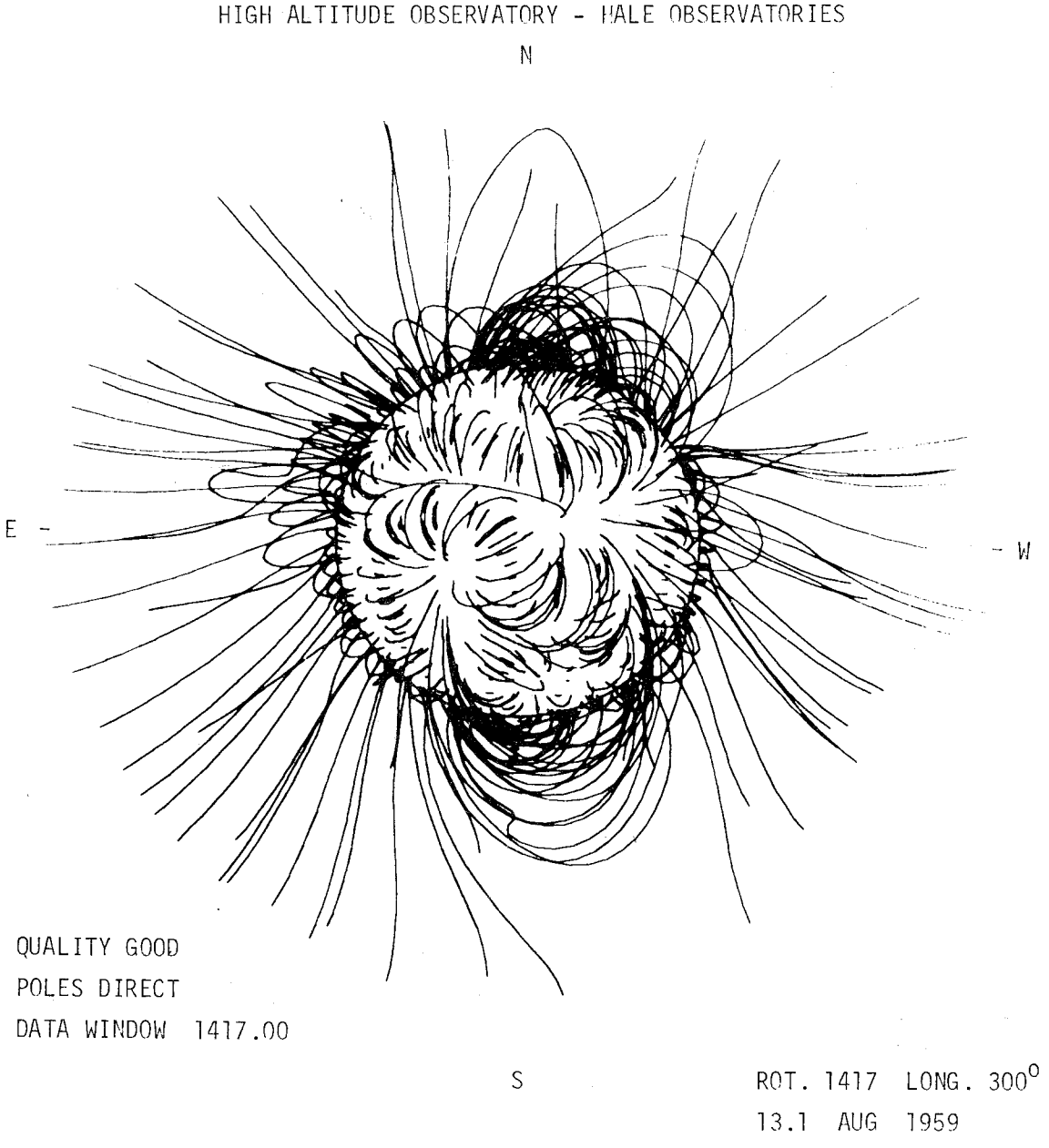

Figure 1. The geometry of the coronal magnetic field from 1.03 R to 2.5 R is displayed in the general field maps.

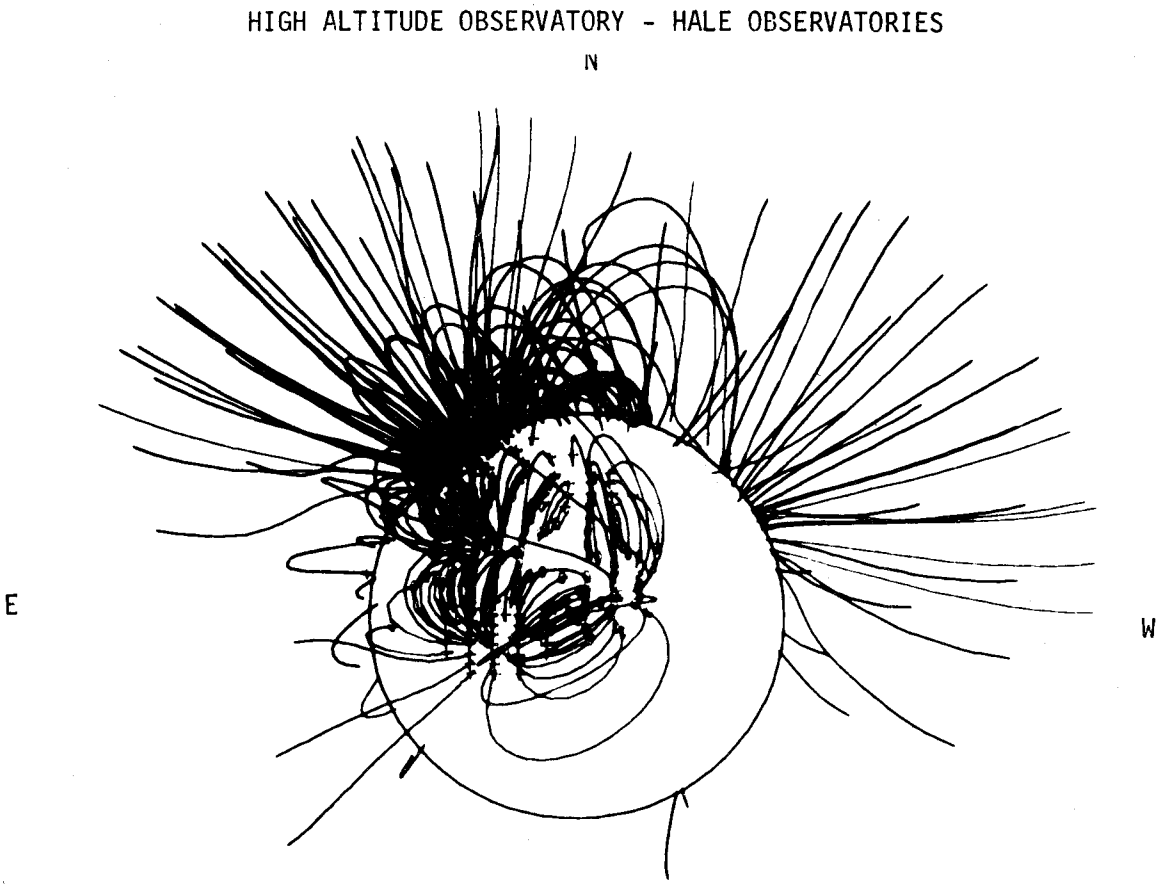

Figure 2. Strong-field maps plot field lines which emanate from the photospheric regions of strongest magnetic field. The 2592 equal-area elements of a photospheric network are ranked in terms of magnetic field strength, and 400 field lines are plotted from those area elements of greatest field strength.

line was used. After July 12, 1966, the scanning aperture dimensions were 17 arcsec x 17 arcsec. The equipment, the observational techniques, and the methods of reduction are described by Howard, et al., (1967). The data and the maps derived from them may be conveniently divided into two epochs: (1) that of the Atlas of Solar Magnetic Fields (Howard, et al., 1967) covering the period from August 1959 to July 1966, and (2) that of the daily (and now digitized) magnetograms covering the period August 1966 to June 1970.

For the calculation of the maps contained in this Atlas the photosphere was divided into 1080 surface elements of equal area, with 30 zones ($\Delta \sin \lambda = 0.0667$, in latitude λ) and 36 sectors ($\Delta\phi = 10^{o}$, in longitude ϕ). The Mt. Wilson line-of-sight magnetograph data were averaged for each surface element. Corrections for magnetograph saturation were then added to the relevant surface elements (as explained in Section 10 of Paper I). The average line-of-sight fields of the 1080 equal surface elements were then used to calculate the Legendre coefficients for the entire photospheric magnetic field (see Section 6 of Paper I).

IV. LIMITATIONS

These calculations of the coronal magnetic field have several limitations which are described in detail in Paper I. They are re-examined below to aid the reader in applying the maps to particular problems. Naturally, these limitations arise from the characteristics of both the theoretical model and the original photospheric data.

A. Current-Free Approximation

Since synoptic magnetic measurements are available only for the longitudinal (line-of-sight) photospheric field, we have no information about large-scale electric currents in the corona. Thus, the assumption is made that the coronal magnetic field is current-free and can be expressed mathematically as the gradient of a scalar (or potential) function which satisfies the Laplace equation. There is some evidence that the magnetic field of the inner corona is very nearly current-free (or potential) (Newkirk and Altschuler, 1970; Rust and Roy, 1971; Dulk et al., 1971). However, near active regions and prominences this assumption undoubtedly breaks down although we have no information as to the extent of the electric currents and their influence on the large scale coronal magnetic fields. Moreover, evolutionary changes in the photosphere and transient events such as flares and surges may induce coronal electric currents which will modify the magnetic field. Hopefully, these maps of the ambient current-free coronal field will serve as a tool for the investigation of these fundamental questions.

An ever present departure from the current-free condition is produced by the solar wind, which drags the magnetic field into essentially a radial direction beyond about 2R (where R = 1 solar radius) and, by distorting magnetic field lines, induces a volumetric and sheet current system. Thus, a complete analysis of the coronal magnetic field, including the dynamics of the solar wind, would require the numerical solution of a complicated set of nonlinear partial differential equations (Pneuman and Kopp, 1970). Since

such a solution is currently not available for the degree of complexity represented by the coronal fields, we simply adopt the approximation in this Atlas that the coronal magnetic field becomes radial on some sphere of radius R_W. This is achieved by setting the scalar (or potential) function equal to zero at this radius. In Figure 3 we compare the field geometry of a simple dipole field distorted by the solar wind as given both by the detailed calculation of Pneuman and Kopp (1970) and by our approximation. Within the region of application of our zero-potential solution, the agreement between these two calculations appears adequate for practical purposes.

The choice of the value of R_W has evoked considerable discussion. Schatten et al. (1969) found $R_W \approx 1.6$ R from the average magnitude and frequency spectrum of the fields measured at 1 AU while Altschuler and Newkirk (1969) used $R_W = 2.5$ R to bring about the best fit between the shapes of the field lines and the structures observed in the corona at the eclipse of 1966. Since we now know that because of the filamentary nature of the photospheric field, its strength had been underestimated by a factor 1.8 (Howard and Stenflo, 1972), the larger value of R_W now appears compatible with both the eclipse observations and the magnitude of the interplanetary field.

Our solution of Laplace's equation and the maps give the field only between $1R \leq r \leq 2.5R$. To map the magnetic field of the outer corona ($r > 2.5$ R), Schatten (1971) has suggested that

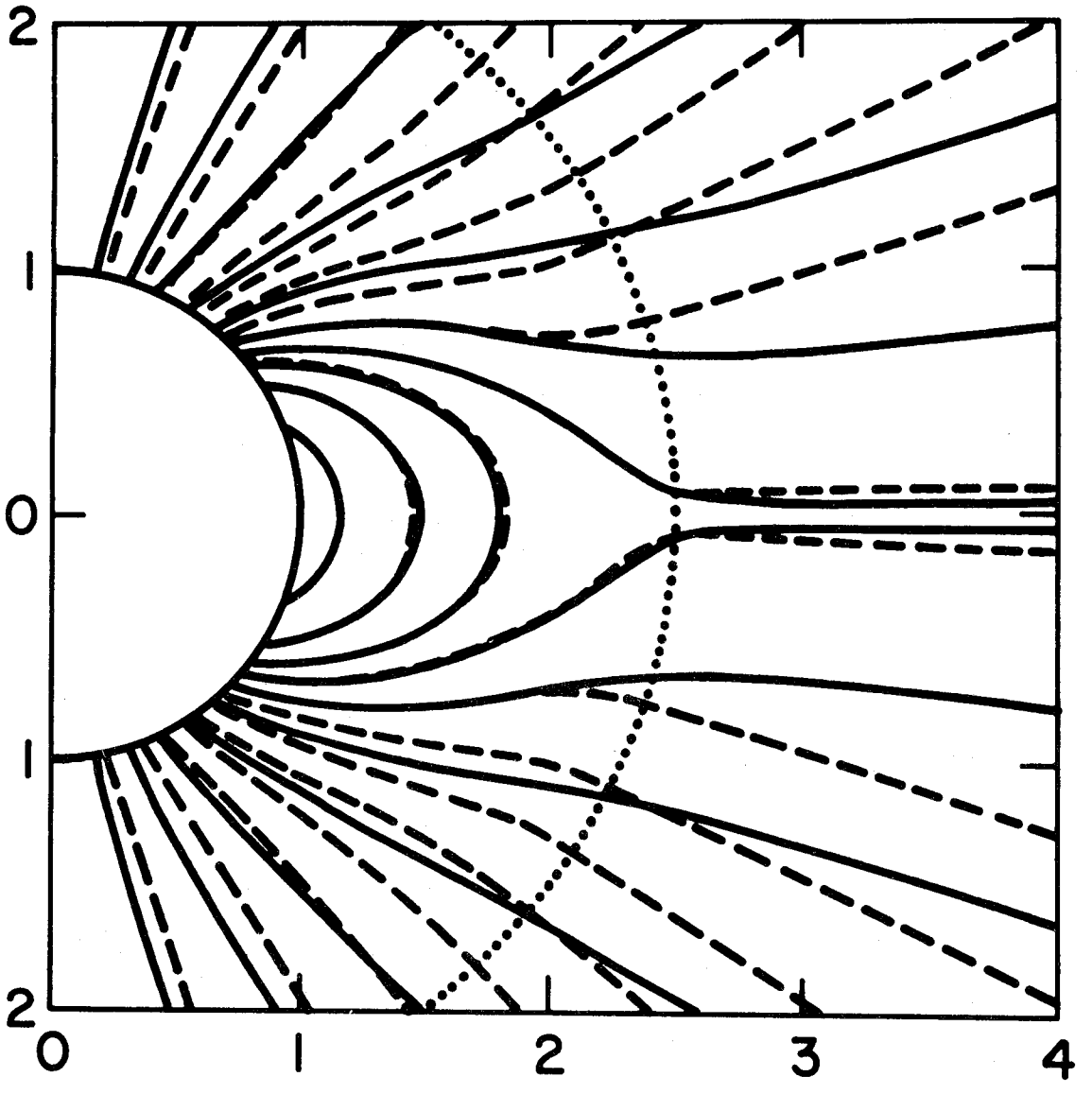

Figure 3. Comparison of the shapes of coronal magnetic field lines calculated for a dipole surface field according to Pneuman and Kopp (1971) (solid lines) and for a potential field (dashed lines) with a zero-potential surface at R_w. The zero-potential solution is not valid above R_w (dotted arc). Foot points for high-latitude field lines are separated for clarity. The super-Alfvenic point in the exact solution occurs at 2.56 R_o in the streamer.

the outer field, although distorted by the solar wind (and thus containing electric currents) corresponds in magnitude and geometry (but not field direction) to a potential (current-free) field which would arise if all the magnetic flux at r = 2.5 R has the same magnetic polarity (i.e. monopolar). Schatten's minimum energy magnetic configuration for the outer corona has not been included in this computation.

B. Truncation of the Polynomial Series

Since the number of polynomials used to approximate the field is necessarily limited, the influence of truncating the expansion must be examined from the standpoints of both the stability of the lower order polynomials as well as the imposed limit on spatial resolution.

The stability of the dominant, lower order polynomials may be tested by comparing the power

$$S_n = \sum_{m=0}^{n} \left[(g_n^m)^2 + (h_n^m)^2 \right]$$

of index n for different truncation limits N = max(n). Here the orthonormalization condition is

$$\frac{1}{4\pi} \int_{\theta=0}^{\pi} \int_{\theta=0}^{2\pi} P_n^m(\theta) \begin{Bmatrix} \cos m\phi \\ \sin m\phi \end{Bmatrix} P_{n'}^{m'}(\theta) \begin{Bmatrix} \cos m'\phi \\ \sin m'\phi \end{Bmatrix} \sin\theta \, d\theta \, d\phi = \delta_{mm'} \, \delta_{nn'} \, .$$

The accompanying table compares the power S_n for $1 \leq n \leq 5$ for N = 5, 7, and 9 for three typical dates during the period covered

by the Atlas. The index n corresponding to the maximum value of S_n is indicated by an asterisk. The percent change of $\max(S_n)$ when the principal index is increased from 5 to 9 is less than 10%. The percent change of the actual harmonic coefficient (roughly the square root of the power) and thus of the calculated field is half of this. Thus, for practical purposes, the values of the harmonics of low n are not greatly affected by the truncation of the series expansion. This result is reasonable because the matrix to be inverted when solving for the least-mean-square solution is largely diagonal.

Values of the Power S_n

n \ N	5	7	9	max change (%)
	12 Nov 1966			
1	6.93 (-3)	7.02 (-3)	6.44 (-3)	9 *
2	1.28 (-3)	1.36 (-3)	1.42 (-3)	10
3	2.00 (-3)	1.94 (-3)	2.13 (-3)	4
4	1.55 (-3)	1.25 (-3)	1.36 (-3)	23
5	1.07 (-3)	0.95 (-3)	1.04 (-3)	12
	7 Mar 1970			
1	4.53 (-2)	5.31 (-2)	4.37 (-2)	22
2	8.83 (-2)	9.00 (-2)	9.06 (-2)	3
3	13.03 (-2)	13.02 (-2)	13.32 (-2)	2 *
4	5.20 (-2)	4.88 (-2)	4.79 (-2)	9
5	4.74 (-2)	4.29 (-2)	4.32 (-2)	10
	21 June 1970			
1	5.23 (-2)	5.76 (-2)	5.24 (-2)	10
2	2.65 (-2)	2.57 (-2)	2.75 (-2)	7
3	8.33 (-2)	7.83 (-2)	8.47 (-2)	8 *
4	2.25 (-2)	2.13 (-2)	2.35 (-2)	9
5	3.61 (-2)	3.47 (-2)	3.49 (-2)	4

* Indicates Dominant Multipoles

The spatial resolution of the maps is limited both by the original data and by the value of N. To determine the Legendre coefficients, the surface field is averaged in 1080 elements of equal area, thereby limiting the maximum obtainable resolution of magnetic features to 10^{o} in longitude and $\Delta \sin \lambda = 0.0667$ in latitude. However, since the Legendre polynomial is truncated at a principal index of N = 9, the actual resolution is somewhat less. Thus, comparison of the fields indicated on these maps with small phenomena, such as prominences and small coronal structures, may be misleading.

C. Limited Data Coverage

The Mt. Wilson data are the only full solar disk magnetic measurements continual over a long period of time, and thus, the only data suitable for the production of such an Atlas. However, these measurements are restricted to one magnetic component (line-of-sight), to one atmospheric level (the photosphere), and to a relatively small intensity range (from about 0.5 to 100 Gauss). Also, because of foreshortening effects, the magnetograph measurements are representative of actual fields only near the center of the visible solar disk, that is, for latitudes within about 45^{o} from the solar equator and for longitudes within three days of central meridian passage. Thus, photospheric magnetic data at the poles are of limited accuracy, and data covering the entire sun must be collected over at least one complete solar rotation. As a result, any magnetic field fluctuations in the photosphere which have time scales shorter than a solar rotation are not represented and may introduce errors. This, as well as other

unavoidable errors in measuring the photospheric field over an entire solar rotation, causes a spurious net monopole component for the solar field. This spurious monopole contribution can be removed by adding a constant to all the line-of-sight field measurement as described in Section 6 of Paper I: this procedure corresponds to a systematic calibration of the line-of-sight field data. The resulting field has no monopole component larger than one part in 10^8.

When data were available for the same position on the sun for several days around central meridian passage, a weighted average was taken to obtain the best value for the line-of-sight magnetic field of the region at central meridian. The data therefore, give the line-of-sight component of the poloidal photospheric field. From the daily magnetic maps one could also determine an average value for the azimuthal field component at each point on the solar surface. In practice, day to day fluctuations in the magnetic field are large enough to make any estimate of the azimuthal field unreliable; thus, the additional effort in data reduction to include the azimuthal field cannot be justified (Harvey, 1969).

D. Magnetograph Saturation

Because of the shape of the line profile, the Mt. Wilson magnetograph signal begins to saturate at about 100 Gauss, and the flux from regions of high field strength may be underestimated. Thus, the magnetograph data may indicate a spurious net magnetic

flux through the active region which may noticeably affect the validity of the calculated coronal field pattern. To avoid a large spurious flux from active regions, it is necessary to include data concerning the high intensity magnetic fields of sunspots.

The most extensive study of the magnetic flux in active regions has been carried out by Stenflo (1967) who concludes that if both weak and strong fields of both magnetic polarities are considered in an active region, the flux imbalance amounts to only 5 to 10% of the total flux. Stenflo's data for eleven active regions were used to determine a statistical correction for the spurious flux arising from the magnetograph saturation (cf. Section 10 of Paper I). The correction, applied to the Mt. Wilson measurement of the field of an active region, uses the maximum field strength and polarity of the preceding sunspot as measured by the Crimean Astrophysical Observatory.

It must be emphasized that the correction is statistical and may be wrong in magnitude and sometimes even in sign. From a new analysis based on the work of Howard and Stenflo (1972) Stenflo suggests that the correction we used should be multiplied by a factor of 0.38. Figures 4, 5, and 6 show (flux-proportional) stereo maps all calculated from the same Mt. Wilson data (1) with no correction for saturation ($c = 0$), (2) with the correction for saturation used in this Atlas ($c = 1$), and (3) with the newly suggested correction ($c = 0.38$), respectively. For most purposes,

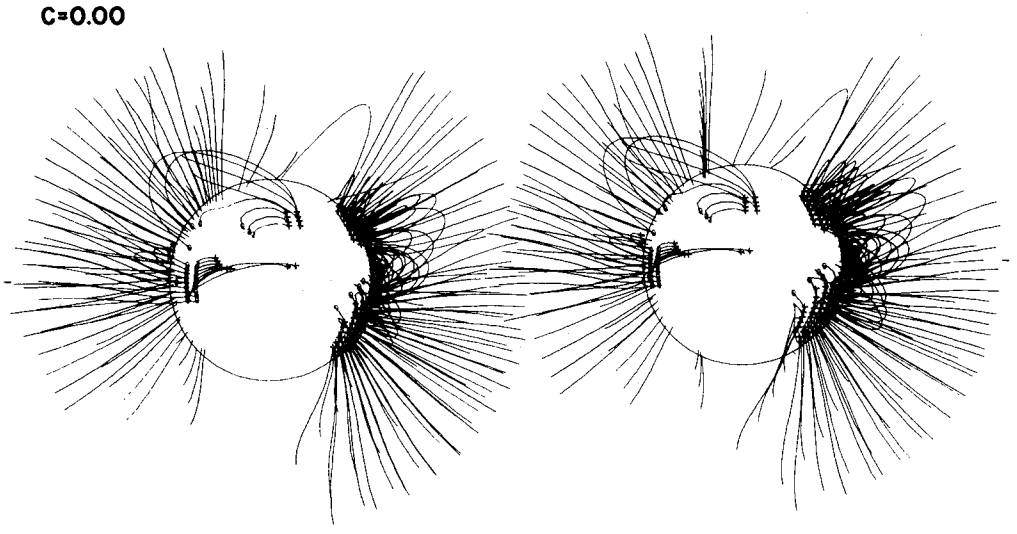

Figure 4. Strong field stereographic maps of the field with no correction for magnetograph saturation.

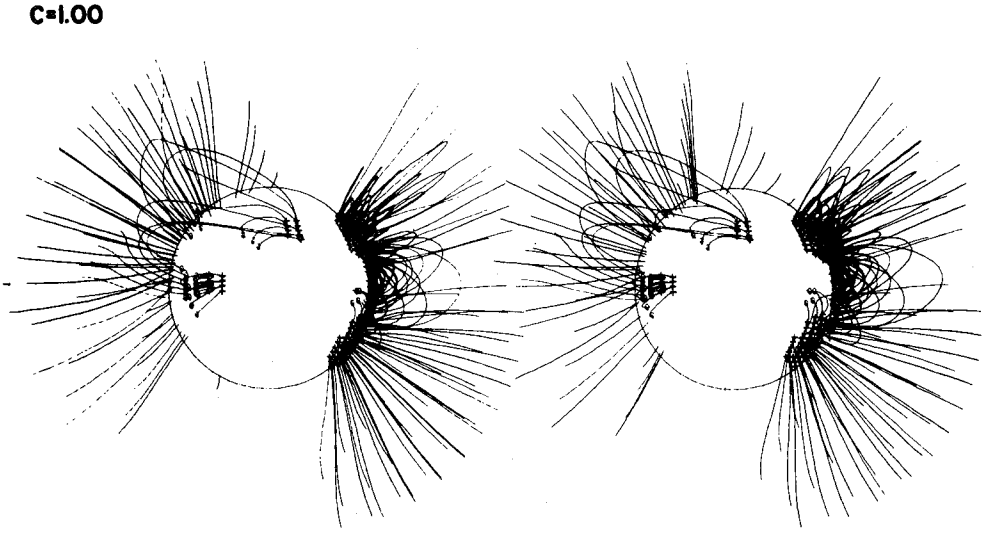

Figure 5. Strong field stereographic maps of the field with correction for magnetograph saturation as described in Section 10 of Paper I and as used in this Atlas.

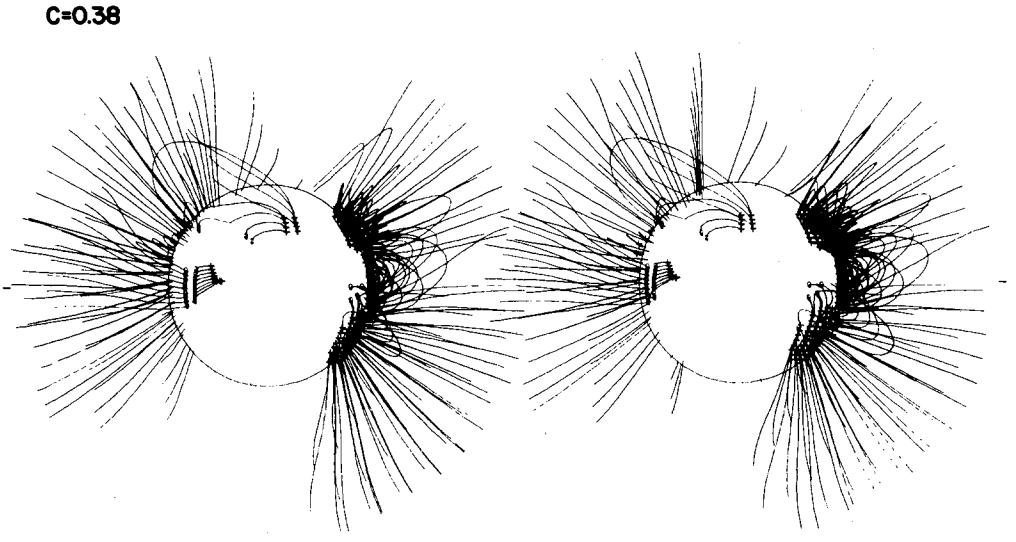

Figure 6. Strong field stereographic maps of the field with correction for magnetograph saturation as suggested by Howard and Stenflo (1972).

there is no important difference between the maps using c = 1 and those using c = 0.38.

E. Polar Fields

The difficulty of obtaining magnetic data near the poles requires special comment. Because of the line-of-sight projection, polar magnetic data are less accurate than data of magnetic fields at lower latitudes. During one extended period covered by this Atlas, the line-of-sight magnetic field was not reported in the routine magnetograms for latitudes exceeding 40^{o}. For this period, a mean "polar field" for each 120^{o} in longitude and for latitudes above 60^{o} was estimated by Howard (1972). The photospheric field between 40^{o} and 60^{o} latitude for each sector of longitude was then determined by interpolating along the meridian between the measured field at (the surface element of) 40^{o} latitude and the estimated field at (the surface element of) 60^{o} latitude.

We naturally ask what influence this uncertainty in the polar fields (particularly during the period when the polar field was not directly measured) has on the calculated coronal maps. First, we note that during the interval when the polar field was not directly measured, the polar fields were, in fact, weak and thus contributed much less magnetic flux to the coronal field than did the photospheric regions at lower latitudes. However, gross errors in the polar fields, which would lead to a spurious net monopole flux from the sun, are removed in the computer program. Thus, even during the period when the polar field was not directly

measured, the coronal fields calculated for latitudes below 40^{o} should be accurate. The gross structure of field lines connecting lower latitudes to the polar regions should still be fairly representative of the true situation, although the details of such field configurations whenever averaged polar data were used or when unusually strong polar fields are indicated should be treated with caution.

V. USING THE ATLAS

The north-south axis oriented vertically on each map is the rotation axis of the sun. Thus, each map presents the appearance of the sun as viewed by an observer in the solar equatorial plane. The rotation number and the longitude of the central meridian are the Carrington designation given in the American Ephermeris and Nautical Alamanac. The Atlas contains two field maps for every 10^{o} of longitude in the Carrington system. The calculation of a given field line is begun at r = 1.03 R and is traced using a Runge-Kutta technique in steps of 0.1 R until the field line either returns to the solar surface or reaches the radius of zero potential (r = 2.5 R).

For the first or "general field" map, the solar surface (photosphere) is divided into 648 surface elements of equal area ($\Delta \sin \lambda = 0.0833$ in latitude and $\Delta\phi = 13^{o}.3$ in longitude, thus 24 x 27 elements of equal area). A field line is plotted from the center of any surface element whenever the calculated field strength at the photosphere exceeds the minimum value of 0.08 Gauss. As many as 648 field lines can be plotted, thereby sampling the magnetic field of the entire solar corona. Thus, the first map shows the overall geometry of the current-free (potential) magnetic field consis-

tent with the photospheric magnetic data, but does not distinguish strong from weak field regions. Since the starting footpoint of each field line is located at the centroid of a surface element, a map may show a group of field lines whose footpoints are perfectly aligned. Such perfect alignment of the footpoints of the field lines should be considered as an artifact of the representation; the magnetic geometry shown in the map, however, is correct.

For the second or "strong field" map, the solar photosphere is divided into 4 x 468 = 2592 surface elements of equal area ($\Delta \sin \lambda = 0.0417$ in latitude and $\Delta\phi = 6^{o}.75$ in longitude). In this case, the fields at the centroids of all 2592 elements are calculated and ranked according to field strength. Field lines are drawn from the 400 surface elements with the strongest calculated field strength. Thus, this map plots only 15% of the possible field lines and shows the coronal field lines originating at the photospheric regions of strongest magnetic field.

We note that the coefficients for the Legendre series solution of the Laplace equation were derived from photospheric magnetic measurements (or interpolations) at 1080 surface elements of equal area. Although the general-field map plots field lines from at most 648 surface elements, the strong-field map plots lines from 2592 surface elements. Thus, in the case of the strong-field map, the larger number of plotted field lines emphasizes the coronal influence of the regions of strong photospheric field but does not represent an improvement in the resolution of the coronal field geometry.

For many purposes, both the strong and general field maps must be consulted. For example, many of the dense coronal regions visible on

X-ray photographs appear to correspond well to the fields represented by the strong field maps while coronal streamers, which may not always be rooted in regions of strong photospheric field, may be outlined by the fields portrayed in the "general field" maps.

The direction of the magnetic field is indicated on the strong field maps. A "+" near the footpoint of a field line means an inward directed (negative or south polar) field. A "0" means an outward directed (positive or north polar) field.

To examine the three-dimensional pattern of the field lines it is convenient to view the maps stereoscopically. To do this, take any two maps separated by 10^{0} in longitude and set the map with higher central meridian longitude on the right.

Each frame of the Atlas contains information in legends below the map:

> QUALITY is a subjective estimate made by one of us, (R.H.) of the quality of the Mt. Wilson magnetograph data for the data period of the map in terms of good, fair, and poor. If there were equal periods of good and fair data contributing to a given map, the rating is conservatively listed as fair. No attempt has been made to compare every map with other solar data such as plages or to evaluate the effects of changes in the photospheric fields on the accuracy of the coronal maps. Rapid changes in the overall pattern of the photospheric field from one rotation to the next could jeopardize the applicability of the coronal maps even though the data for each rotation may be of good quality.

POLES indicates whether direct magnetic measurements of the polar regions (direct) or estimates of the mean polar fields (averaged) were used.

DATA WINDOW gives the leading edge (or earliest date) in Carrington Rotation number of the data set from which the coefficients and the field map were derived. All frames containing the same data window designation are derived from the same set of data. For example, data window 1417.00 means the data panel spans 360^{o} of longitude with data extending from rotation 1417 longitude 350^{o} through rotation 1417 longitude 0^{o}. (The longitude sectors are designated by the eastern edge; hence, longitude 350^{o} indicates the sector spanning 350^{o} to 360^{o}.)

ROTATION and LONGITUDE indicate the central meridian of the sun in the Carrington system for the map presented. The corresponding DATE is presented in universal time to a fraction of a day.

Whenever the data were so incomplete that it was not possible to determine the average line-of-sight field for surface elements along certain meridians or over some longitudinal extent, no map was calculated. Thus, there are time periods between August 1959 and June 1970 for which no maps are included in this Atlas. Such periods are indicated throughout the Atlas film by special frames labelled "NO OBSERVATIONS" which are

separated from the adjacent field maps by blank frames. The special frames delineate the periods of missing data in terms of rotation numbers, longitudes, and dates. For example, a frame reading

NO OBSERVATIONS

Rot. 1418 Long. 230 - Rot. 1418 Long. 120

14.0 Sep 1959 - 23.0 Sep 1959

means that twelve field maps of each type are missing because adequate surface data did not exist. Since we designate a 10^{o} sector by the longitude of its eastern (or following) edge, in the above example no data existed from longitude 240^{o} through longitude 120^{o}.

VI. EXTENSIONS OF THIS ATLAS

For many investigations the simple representations of the coronal magnetic field which appear in this Atlas are insufficient. For example, it may be desirable to combine quantitative information on the field with other coronal parameters in a detailed computation. Inquiries concerning such analyses should be directed to any of the authors.

REFERENCES

Altschuler, M. D., and G. Newkirk Jr., 1969: Magnetic fields and the structure of the solar corona. I. Methods of calculating coronal fields. *Solar Phys. 9*, 131-149.

Bohlin, J. D., 1970: Solar coronal streamers. II. Evolution of discrete features from the sun to 1 AU. *Solar Phys. 13*, 153-175.

Dulk, G. A., and M. D. Altschuler, 1971: A moving Type IV radio burst and its relation to the coronal magnetic field. *Solar Phys. 20*, 438-447.

———, ———, and S. F. Smerd, 1971: Motion of Type II radio burst disturbances in the coronal magnetic field. *Astrophys. Lett. 8*, 235-239.

Harvey, J. W., 1969: Private communication.

Howard, R., 1972: Polar magnetic fields of the sun: 1960-1971. *Solar Phys. 25*, 5-13.

———, and J. O. Stenflo, 1972: On the filamentary nature of solar magnetic fields. *Solar Phys. 22*, 402-417.

———, V. Bumba, and S. F. Smith, 1967: *Atlas of Solar Magnetic Fields 1959-1966*, Carnegie Institution of Washington Publication No. 626.

Lantos-Jarry, M. F., 1970: Coronal magnetic field patterns inferred from radio observations. *Solar Phys. 15*, 40-47.

Martres, M., M. Pick, and G. K. Parks, 1970: The origin of interplanetary sectors from radio observations. *Solar Phys. 15*, 48-60.

McCabe, M. K., 1971: Mass motions in a flare spray. *Solar Phys. 19*, 451-462.

Newkirk, G., 1971: Large scale solar magnetic fields and their consequences. In *Solar Magnetic Fields* (R. Howard, Ed.), Proc. of IAU Symposium No. 43, Paris, 547-568.

———, and M. D. Altschuler, 1970: Magnetic fields and the solar corona. III. The observed connection between magnetic fields and the density structure of the corona. *Solar Phys. 13*, 131-152.

———, ———, and J. W. Harvey, 1968: Influence of magnetic fields on the structure of the solar corona. In *Structure and Development of Solar Active Regions* (K. O. Kiepenheuer, Ed.), Proc. of IAU Symposium No. 35, D. Reidel Publ. Co., Dordrecht, 379-384.